2018-10-01

Community managed forests dominate the catchment sediment cascade in the mid-hills of Nepal: A compound-specific stable isotope analysis.

Upadhayay, HR

10.1016/j.scitotenv.2018.04.394
Science of the Total Environment
Elsevier

Title

Community managed forests dominate the catchment sediment cascade in the mid-hills of Nepal: a compound-specific stable isotope analysis

Hari Ram Upadhayay (1, 4)*, Hugh G. Smith (2), Marco Griepentrog (1, 3), Samuel Bodé (1), Roshan Man Bajracharya (4), William Blake (5), Wim Cornelis (6), Pascal Boeckx (1)

(1) Isotope Bioscience Laboratory - ISOFYS, Faculty of Bioscience Engineering, Ghent University, Coupure Links 653, 9000 Gent, Belgium, (2) Landcare Research, Private Bag 11052, Palmerston North 4442, New Zealand, (3) Biogeoscience, Department of Earth Sciences, ETH Zurich, Sonneggstrasse 5, 8092 Zurich, Switzerland, (4) Aquatic Ecology Center (AEC), School of Science, Kathmandu University, Dhulikhel, Nepal, (5) School of Geography, Earth and Environmental Sciences, Plymouth University, Plymouth, Devon, PL4 8AA, UK, (6) Soil Physics Group, Faculty of Bioscience Engineering, Ghent University, Coupure Links 653, 9000 Gent, Belgium

*Correspondence to:

Hari R. Upadhayay

hariram.upadhayay@ugent.be or hrgene@gmail.com

Phone: +32 9 264 6006; Fax: +32 9 264 6242

Date of acceptance: 29 April 2018

DOI: doi: 10.1016/j.scitotenv.2018.04.394.

Abstract

Soil erosion by water is critical for soil, lake and reservoir degradation in the mid-hills of Nepal. Identification of the nature and relative contribution of sediment sources in rivers is important to mitigate water erosion within catchments and siltation problems in lakes and reservoirs. We estimated the relative contribution of land uses (i.e. sources) to suspended and streambed sediments in the Chitlang catchment using stable carbon isotope signature ($\delta^{13}C$) of long-chain fatty acids as a tracer input for MixSIAR, a Bayesian mixing model used to apportion sediment sources. Our findings reveal that the relative contribution of land uses varied between suspended and streambed sediment, but did not change over the monsoon period. Significant over- or under-prediction of source contributions could occur due to overlapping source tracer values, if source groups are classified on a catchment-wide basis. Therefore, we applied a novel deconvolutional framework of MixSIAR (D-MixSIAR) to improve source apportionment of suspended sediment collected at tributary confluences (i.e. sub-catchment level) and at the outlet of the entire catchment. The results indicated that the mixed forest was the dominant (41 ± 13%) contributor of sediment followed by broadleaf forest (15 ± 8%) at the catchment outlet during the pre-wet season, suggesting that forest disturbance as well as high rainfall and steep slopes interact for high sediment generation within the study catchment. Unpaved rural road tracks located on flat and steep slopes (11 ± 8 and 9 ± 7% respectively) almost equally contributed to the sediment. Importantly, agricultural terraces (upland and lowland) had minimal contribution (each <7%) confirming that proper terrace management and traditional irrigation systems played an important role in mitigating sediment generation and delivery. Source contributions had a small temporal, but large spatial, variation in the sediment cascade of Chitlang stream. D-MixSIAR provided significant improvement regarding spatially explicit sediment source apportionment within the entire catchment system. This information is essential to prioritize implementation measures to control erosion in community managed forests to reduce sediment loadings to Kulekhani

hydropower reservoir. In conclusion, using compound-specific stable isotope (CSSI) tracers for sediment fingerprinting in combination with a deconvolutional Bayesian mixing model offers a versatile approach to deal with the large tracer variability within catchment land uses and thus to successfully apportion multiple sediment sources.

Keywords

fatty acids, compound-specific stable isotope (CSSI) analysis, isotope mixing model, deconvolutional approach, MixSIAR

1 Introduction

Soil erosion by water is of paramount importance for Nepal because of its adverse impacts on soil quality (Acharya et al., 2008; Gardner and Gerrard, 2003), aquatic life in lakes and rivers, and reservoir capacity (GoN/EbA/UNDP, 2015). Degradation of soils through water erosion is one of the key issues affecting agriculture in the mid-hills of Nepal (Acharya et al., 2008; von Westarp et al., 2004). Therefore, it is also considered a major threat to food security and potentially puts rural mountain communities, which rely on the economy of local agriculture and subsistence farming, at risk. Moreover, river, lake and reservoir siltation represent a major challenge and its effect can be environmentally and economically detrimental in terms of water and energy security of the region (GoN/EbA/UNDP, 2015). Human activity, combined with natural factors such as steep slopes, fragile geology and intensive monsoon rains, provides conditions for extensive soil loss and is intrinsically linked with catchment degradation. Given the complex interaction with human activities and environment, the nature and extent of soil erosion is highly variable in space and time. Upstream erosion control such as improvements in terracing, low-till agriculture and reforestation have been the focus to mitigate erosional losses (Tiwari et al., 2009) and to reduce sedimentation of reservoirs and lakes in the mid-hills of Nepal. However, questions remain about the extent to which specific land-use types prevent or exacerbate erosion and land degradation in the context of current and future projected agricultural intensification (Bahadur, 2012) as well as changing rainfall patterns in the mid-hills of Nepal (Bookhagen, 2010). Answering these questions is critical to developing a strategy for preventing soil loss and reducing siltation of lakes and reservoirs.

Information on land use-based sediment sources can considerably enhance our understanding of sediment origin. Sediment source fingerprinting by compound-specific stable isotope (CSSI) analyses of fatty acids (FA) has been used as a reliable method to

investigate land use-based sediment sources at the catchment scale (Gibbs, 2008; Upadhayay et al., 2017). The premise of the CSSI sediment source fingerprinting approach is that soil from different land uses can be distinguished based on isotopic composition (^{13}C) of FAs bound to soil particles (Gibbs, 2008; Upadhayay et al., 2017). Fatty acids are biosynthesized by higher plants, delivered to soils and thereby labelling the soil with FAs having a specific $\delta^{13}C$ signature ($\delta^{13}C$-FAs). Fatty acids associated with soil particles, get mixed during downstream sediment transport. Isotope mixing models using $\delta^{13}C$-FA values of sources and sediment sinks offer the possibility of estimating the relative contribution of sources to the sediment (Upadhayay et al., 2017). These estimates can be used to identify differences in sediment sources on spatial (e.g. sub-catchments) and temporal (e.g. seasons) scales and to suggest catchment remediation measures (Mukundan et al., 2012).

Sediment fingerprinting has been successfully applied as a tool to gain insights into sediment dynamics at a river basin scale in catchments all over the world since the 1970s (Mukundan et al., 2012; Walling, 2013). Spatio-temporal variation of sediment source apportionment has received increasing attention (Cooper et al., 2015; Vale et al., 2016; Vercruysse et al., 2017), because primary sediment sources are site-specific and vary within a catchment (Koiter et al., 2013a; Stewart et al., 2015). In essence, changes in rainfall pattern and intensity, and land cover change in both natural (e.g. loss of leaf cover in a deciduous forest during winter) and agricultural systems (e.g. bare soil due to changing cropping patterns) cause marked temporal variations in sediment sources and dynamics (Merz, 2004). Often the fingerprinting signature of different land uses (sources) is only weakly expressed by the applied tracer techniques (Pulley et al., 2017). A possible solution lies in alternative sampling approaches, such as (1) 'compositional evolution' (Hardy et al., 2010), whereby sources, as well as sediment, are sampled along the river, or (2) 'confluence-based sediment fingerprinting' (Vale et al., 2016), whereby upstream sediment samples are taken as a proxy

for sub-catchment sediment signature in order to evaluate relative source contributions for larger catchments. The former approach does not account accurately for sub-catchment contributions as well as local variability of tracers, while the latter approach lacks the ability to provide information on the specific sediment sources within sub-catchments (Vale et al., 2016). Very limited work has been done to identify land use-based sediment sources and to estimate their relative contributions as a function of land use within sub-catchments using CSSI tracers. In this study, we applied the CSSI sediment source fingerprinting approach within a representative catchment and its sub-catchments in the mid-hills of Nepal. The objectives were (a) to determine the relative contributions of generic sediment sources (i.e. catchment-wide source groups) to sediment loads and (b) to evaluate how source contributions to the catchment sediment cascade change on a spatio-temporal basis.

2 Material and methods

2.1 Catchment description

The study was conducted in the Chitlang catchment (23 km^2), which drains into the Kulekhani Hydropower Reservoir (also known as Inra Sarobar), located in the mid-hills of Nepal (Fig. 1). This catchment is mainly dominated by forests (>70%), which can be categorized into broadleaf forest (25%), mixed forest (40%) and pine forest (6%) (Table A.1). The agricultural systems consist of (a) lowland terraces (6%): bunded irrigated levelled terraces called “Khet” and (b) upland terraces (23%): unbunded rain-fed levelled terraces called “Bari”. Rice is predominantly grown in lowland terraces during the peak monsoon season (July to September). Wheat and other commercial vegetables are dominant during the winter season in the lowland terraces. Similarly, in the upland terraces, maize may be grown as a monoculture or intercropped with finger millet and other vegetables (potato, cabbage, cauliflower, legumes). Most cropland is either privately owned or rented and receives

151 inorganic fertilizer and farmyard manure, while forests are owned and managed by
152 community forest user groups (CFUs).

153 The catchment has a rugged terrain with an elevation ranging from 1515 to 2555 m and
154 an average slope gradient of 44% (Fig. 1b and Fig. 2a). Less than 27% of the area has a slope
155 <30%. Land use is closely related to the slope gradient of the catchment (Fig 1). Slopes <25%
156 are dominated by agriculture, while lowland terraces are found particularly at the bottom of
157 the hills on relatively flat land (<15% slope gradient) near stream banks (Fig. 1b). Forests
158 dominate on steeper slopes (>25%). The catchment is characterized by monsoon climate, with
159 two distinct seasons: summer monsoon and dry winter (Fig. 3). Annual average precipitation
160 is ~1750 mm (maximum 2386 mm and minimum 1182 mm according to data from 1980 to
161 2015). Most precipitation (circa 77%) occurs during the peak monsoon season between June
162 and September (Markhu Gaun station (index no 0915), Department of Hydrology and
163 Meteorology (DHM), Government of Nepal). Additionally, 16% of precipitation occurs in
164 early (April and May) and late monsoon (October and November) and 7% during the dry
165 winter period (between December and March).

166 The soils in the catchment are classified as Cambisol (Dijkshorn and Huting, 2009)
167 developed on Phulchoki sub-group which consists of Chitlang (dominant in the headwaters),
168 Chandragiri, Sopyang and Tistung formation (Dhital, 2015). Surface soil has a silt-loamy
169 texture with significantly higher soil erodibility (K) on cropland compared to forest land
170 (Upadhayay et al., 2014). However, average surface soil loss from cropland with gentle slopes
171 of 14-20% is estimated to be below 2.5 t ha^{-1} yr^{-1} (Sthapit and Balla, 1998). Water erosion
172 supplies sediment to the 9.7 km long Chitlang stream (drainage density: ~ 4.1 km km^{-2}) and to
173 the Kulekhani reservoir (Fig 1a). This reservoir is of national importance as it is the only
174 functional seasonal reservoir of Nepal and provides 25-30% of the national electricity demand

during the dry season (NEA, 2016). The Kulekhani reservoir lost circa 40% of its water storage capacity in 30 years of operation due to siltation (Shrestha, 2012).

2.2 Source soil and sediment sampling

Potential sediment sources and sediment sampling locations were identified via a land use map digitized from *Google Earth* and a topographical map obtained from the Department of Survey, Government of Nepal as well as a reconnaissance survey in 2013. Identified land-uses were divided into five generic potential sediment source (primary) groups: broadleaf forest (BLF), mixed forest (MF), pine forest (PF), upland terraces (UP) and lowland terraces (LL) (Fig. 1a, Table A.1). Unpaved road tracks (RT) were considered as secondary sediment source since RT do not generate carbon isotopic signature, but rather integrate the signatures of the adjacent land uses. The sampling strategy was designed to take the distribution of land uses, especially the patchy agricultural practices (i.e. smallholder farmers with great variability in crop choice, agronomic practices and inputs) across the catchment, topographic locations and sub-catchments into account. Multiple composite soil samples from different spatial locations belonging to each land use were obtained according to natural and management factors, and accessibility. Each composite soil sample was composed out of a pool of 15 random subsamples (2 cm top soil obtained using a stainless steel corer with 7.5 cm internal diameter). The composite samples included loose soil in the exposed area as well as fresh deposits at the base of each land use clearly showing recent movement of soil due to overland flow. In case of RT, source samples were taken from their surface and in road-side channels. Stream-banks were not sampled as a separate source because of high gravel and boulder content dominating the substrate as well as a high vegetation cover along the Chitlang stream and its tributaries (Fig. A.1). Landslides were not observed in the catchment throughout the study period (2013-2015).

Two different types of sediment samples were collected between 2013 to 2015 and 2014 to 2015, i.e. (1) deposited streambed sediment (Fig 2b) and (2) suspended sediment (Fig. 2c), respectively. Both types of sediment samples were retrieved during the early wet (EW; March-May), mid wet (MW; June-August) and late wet (LW; September-October) periods to capture the range of flow conditions that occur over the years and to understand the spatio-temporal variation of sediment sources (Fig. 3). Early wet season is the critical time for soil loss from cropland in the mid-hills of Nepal. Each streambed sediment sample comprised 10-15 subsamples (grabs/scrapings) collected from the floodplain, gabion dam and interstices between larger clasts using a flat trowel over approximately 250 m distance at the outlet (M6) of the catchment (Table 1, Fig. 1a). Suspended sediment was sampled with time-integrated mass-flux samplers (TIMS) (Fig. 2c) that were deployed at specific locations as shown in Fig. 1a. These sediment traps were constructed from PVC pipes (1 m length, 110 mm diameter, following the design of Phillips et al.,(2000). Two replicated sediment traps were installed at each sampling location (except for the outlet, M6, of the Chitlang stream where six replicated TIMS were installed) (Fig.1a). Moreover, suspended sediment was collected up- and downstream of stream confluences to investigate sediment inputs from individual sub-catchments (Fig. 1a, Table 1). Upstream samples were collected very close to (~10 m) the confluence point while downstream samples were collected approximately 200 to 250 m downstream of the confluence.

Additionally, during the rising and falling stages of a large runoff event on 14 to15 August 2014 (116 mm of rain fell over a period of 24 hours), suspended sediment was sampled from bulk water samples into 150 L Nalgene containers at the terminus of the Chitlang stream (M6, Fig. 1a). Sediment was separated by decantation following a settling period in a dark cool room (2-3 days). Additionally, suspended sediment samples were retrieved from TIMS at the outlet of the Chitlang stream covering a duration of 35 days (25

April to 30 May) over a period of 30 aftershocks of local magnitude higher than 5.0 M following the Gorkha earthquake (7.8 M) on 25 April 2015. During this period, the total rainfall was 68 mm with one event having 34 mm rain during less than 24 hours. All soil and sediment samples were air-dried, crushed with a steel roller on a steel tray (Gibbs, 2013) and sieved at 2 mm prior to further analyses.

2.3 Total organic carbon (stable isotope) analysis

Bulk organic carbon contents and stable carbon isotope composition ($\delta^{13}C$) of source soils and sediment samples were measured using an elemental analyser (ANCA-SL, SerCon, Crew, UK) coupled to an isotope ratio mass spectrometer (20-20, SerCon, Crew, UK). A mass of 10 to 15 mg grinded sample was transferred into tin capsules and loaded into an auto-sampler. Wheat flour ($\delta^{13}C$ = -27.21 ± 0.13‰) calibrated against the IAEA-CH-6 standard was used as laboratory standard and stable carbon isotope values were expressed as $\delta^{13}C$ values relative to the Vienna Pee Dee Belemnite (VPDB) international reference standard.

2.4 Fatty acid extraction and carbon isotope measurement

Lipids were extracted from source soils and sediment samples with accelerated solvent extraction (ASE 350 Dionex) using dichloromethane:methanol (9:1, v/v) at 100°C and 1.3×10^7 Pa for 5 min in 3 cycles (30 mL cells, 60 % flush volume). The volume of total lipid extract was reduced by evaporation at reduced pressure and neutral and acidic compounds were separated using solid phase extraction on aminopropyl-bonded silica gel columns according to Blake et al. (2012). The acid fraction was methylated with methanolic HCl (Ichihara and Fukubayashi, 2010) of known carbon isotopic composition ($\delta^{13}C$ = - 40.78 ± 0.33‰) and an internal standard (C_{17} FA, heptadecanoic acid) for FA quantification was added to each sample prior to analysis. Fatty acid methyl esters (FAME) were subsequently analysed by capillary gas chromatography-combustion-isotope ratio mass spectrometry (GC-

C-IRMS; Trace GC Ultra interfaced via a GC/C III to DeltaPLUS XP, Thermo Scientific, Bremen, Germany). FAMEs were identified based on the retention time, while peak purity and confirmation of identity was done using a parallel GC-MS measurement. An in-house prepared FAME mixture (C_{20} - C_{30} FAs), traceable to IAEA-CH6 (cumulative uncertainty on the VPDB scale was < 0.2‰), was injected every six sample injections as a reference for ^{13}C isotope ratio measurement of FAMEs. Sample analyses were run in duplicate or triplicate with a standard deviation lower than 0.4‰. Isotope ratios are expressed as $\delta^{13}C$ values in per mill relative to the VPDB standard. The contribution of the $\delta^{13}C$ values of the added methyl group was subtracted from the $\delta^{13}C$ value of the analysed FAME to determine the $\delta^{13}C$ values of the FAs in the source and sediment samples (see equation in Griepentrog et al., 2015). Cumulative uncertainty on VPDB scale for the FA was < 0.6‰. Long-chain even carbon numbered fatty acids (C_{22} - C_{32}) were used for further analysis.

2.5 Data processing and deconvolutional-MixSIAR formulation

Two tracer sets were defined to evaluate their capacity in discriminating between the potential generic sediment sources (land uses). The first set comprised the $\delta^{13}C$ values of long-chain saturated fatty acids (C_{22}-C_{32}); in the second set, the bulk soil $\delta^{13}C$ value was included together with the $\delta^{13}C$-FA (C_{22}-C_{32}) values. Discriminant analysis (DA) is a supervised statistical algorithm that derives an optimal separation between sources established a priori by maximizing between-source variances while minimizing within-source variance (Huberty and Olejnik, 2006). A prediction matrix was used to assess the performance of DA. A plot of individual scores was used to visualize how the first two discriminant functions (e.g. LD1 and LD2) accounted for separation among land uses. The Mahalanobis distance, a measure of distance between two points in the space defined by two or more correlated

variables, was also used as auxiliary information to evaluate the capacity of tracer sets to discriminate between the land uses.

First, the apportionment of land use sources contributing to sediment was estimated using FA tracers from catchment-wide pooled source groups as input for a concentration-dependent mixing model (pooled-MixSIAR). MixSIAR is a Bayesian isotope mixing model (Stock and Semmens, 2013) for estimating the contribution of end-members (i.e. sources) using the tracer content of sources and sediment with model error (residual and process error) (Parnell et al., 2010; Upadhayay et al., 2017). Before starting the un-mixing process with MixSIAR, conservativeness of the tracers was tested using the point-in-ellipsoid approach (Jackson, 2016). Briefly, a 95% prediction ellipse is made from source tracer data (i.e. 95% of the source data are included in the ellipse) and transformed into a perfect circle, centred around the origin using the covariance matrix. Such transformation was also applied to sediment tracer data points in order to determine whether or not sediment samples are within the radius of the source data circle and are hence conservative. This was done considering all tracers i.e. dimensions in a hyperspace. Subsequently, concentration-dependent MixSIAR was formulated with selected FAs, using a residual error term, with the season (sediment sampling periods) as a fixed effect, and no prior information. A concentration-dependent mixing model is essential for accurate quantification of sediment source contributions (Upadhayay et al., 2018). Residual error accounts for unknown sources of variability in the sediment (Upadhayay et al., 2017). The Markov Chain Monte Carlo (MCMC) parameters in MixSIAR were set as follows: number of chains = 3, chain length = 3,000,000, burn = 1,500,000, thin =500. Convergence of mixing models was evaluated using the Gelman-Rubin diagnostic, rejecting the model output if any variable was above 1.0, in which case the chain length was increased. Furthermore, a diagnostic matrix plot of posterior source contribution was used to evaluate the quality of source discrimination. Mean proportional contributions are reported

along with uncertainty and 90% credible interval (CI). A CI (Bayesian form of confidence intervals) is an interval in the domain of the posterior density function (PDF) used to determine uncertainty, i.e., the probability that the true source contribution lies within the interval.

Second, a novel "deconvolutional MixSIAR" (D-MixSIAR) framework was used to apply land use-based source fingerprinting within the catchment stream network structure. In this approach, sub-catchment-specific sources were first unmixed against sediment from individual tributaries (e.g. M1 and M2, Fig. 1a), and then tributaries were unmixed against sediment after a confluence of both tributaries (e.g. M3, Fig. 1a). Posterior proportional contributions of each basin-wide source were then deconvoluted. This approach allows estimation of the weighted distribution of land use contributions to nested downstream sediment sampling locations. D-MixSIAR requires data input to estimate land use source contributions to stream sediment within each sub-catchment, and the sub-catchment contributions to sediment collected downstream of the confluence of streams draining the sub-catchments. Sediment source apportionment per sub-catchment was done by considering source samples within the contributing sub-catchments, upstream of the suspended sediment collection site. Based on field observations and variability of the CSSI signature, it was decided to subdivide the RT samples from the Dandakharka sub-catchment (Fig. 1a) into sub-groups, namely RT-1 (RT samples from relatively steep areas inside BLF) and RT (RT samples from the flatter part of the catchment), while UP samples comprised sub-group UP and UP-E (= upland agriculture encroached into BLF). All statistical analyses and unmixing modelling were done using R software (version 3.3.1, R Core team, 2016) with SIBER (Jackson, 2016), MASS (Venables and Ripley, 2002), HDMD (McFerrin, 2013) and MixSIAR (Stock and Semmens, 2013) packages in the library.

3 Results

3.1 Discrimination of generic sediment sources

Exploratory statistical analysis to assess the potential discriminative power of applied isotopic tracers is important. Discriminant analysis (DA) based on δ^{13}C-FA shows that the two dimensions accounted for >90% of the variance (LD1 = 57.6%, LD2 = 33.6%) as shown in Fig. 4. Group centroids show multivariate mean values, visualising the separation of source groups relative to the functions. All land use pair-wise Mahalanobis distances from the centroid were highly significant except for the pairs BLF-MF, LL-RT and UP-RT (Table 2). Results showed that BLF-MF was most similar in terms of δ^{13}C-FA values. The discriminant analysis further showed that RT is positioned centrally to all other sediment sources (Fig. 4) with a high spread (Fig. A.2) reflecting the presence of road tracks across different land uses. The classification based on DA allowed for 65% total correct classification with some source groups displaying clear discrimination (e.g. PF), while others with greater similarity in δ^{13}C-FA values proved more difficult to discriminate. The main misclassification is related to the RT, BLF and MF with the lowest correct classification of 11, 45 and 47%, respectively (Table A.2). The inclusion of bulk δ^{13}C into the tracer set did not change the classification accuracy of the sources significantly (data not shown).

3.2 Proportional contributions of different land uses to catchment-wide sediment during monsoon season

Different land use contributions to sediment at the outlet of the Chitlang stream (M6, Fig.1a) were estimated from catchment-wide pooled source groups using MixSIAR (pooled-MixSIAR). Point-in-ellipsoid analysis of isotopic tracers demonstrated that the majority of sediment samples (96 and 94% of suspended and streambed sediment, respectively) fell within the source tracer mixing polygon and hence can be considered as conservative. However, we did not remove any sediment sample that failed the point-in-polygon test in

351 further modelling, since MixSIAR can handle to some extent unknown variations in sediment
352 δ^{13}C-FAs via the residual error term (Semmens et al., 2009; Upadhayay et al., 2017). Mixing
353 modelling results demonstrated the substantial variability and uncertainty in the estimated
354 source contribution to sediment (Fig. A.3) with strong negative correlations in posterior
355 source contribution (Fig. A.4) due to the overlap of tracer values between land uses (Fig. 4,
356 Fig. A.2 a-f) while considering catchment-wide (generic) sediment sources. For example, a
357 very strong negative correlation (-0.97) between the posterior probability of BLF and MF
358 contributions was observed in suspended sediment, while, in the case of streambed sediment,
359 posterior probability distributions of BLF were negatively correlated with MF (-0.57) and RT
360 (-0.54). A negative correlation between posterior probabilities of two sources indicates
361 collinearity and thus a low ability of tracers to discriminate between sources. Furthermore,
362 credible intervals of functionally related sources were wide and overlapping. Therefore,
363 probabilities associated with source contributions were aggregated posteriori, i.e. deciduous
364 forest (DF) was formed from BLF and MF while LL and UP were aggregated to form
365 agriculture (AG), to estimate the proportional contribution of meaningful functional source
366 groups to the different types of sediment i.e. suspended, streambed and events.

367 Figure 5 summarizes the source apportionment results (after aggregating posterior
368 probability of source) of sediment samples that were collected at the outlet (M6) of the
369 Chitlang stream. The estimated mean relative contribution of each source to the suspended
370 sediment indicated that DF was the dominant source during the early, mid and late wet season,
371 with a 90% CI ranging between 90 and 99%, followed by AG ranging between 0.3 and 4%.
372 Similar to the suspended sediment, results for streambed sediment in the Chitlang stream
373 indicated that it was predominantly derived from DF (average contribution of 62, 79 and 68%
374 in early, mid and late wet season, respectively), followed by AG (18, 9 and 15%) and RT (14,
375 5 and 8%) which indicates that surface erosion from agricultural terraces is a minor source

(Fig. 5). For streambed sediment, seasonality was observed for DF with a significantly higher contribution in the mid wet compared to early and late wet-periods (79% versus 62 and 68%, respectively). Source apportionment results did not substantially change in both sediment types i.e. suspended and streambed between the cases where bulk $\delta^{13}C$ was included ($\delta^{13}C$ -FA (C_{22}-C_{32}) + $\delta^{13}C$-bulk) and the cases where bulk $\delta^{13}C$ was not included ($\delta^{13}C$ -FA (C_{22}-C_{32})) as tracer (Fig. A.3). Hence further discussion and conclusions are based on the results of $\delta^{13}C$-FA tracer set.

Additionally, identification and apportionment of sediment sources during intense rainfall events provide the basis for a detailed assessment of critical land uses that contribute substantial amounts of sediment at the catchment scale. Table 3 presents information on the overall mean relative contribution of sources to suspended sediment samples collected at the outlet of the Chitlang catchment during a high rainfall event (14-15 August 2014) and the geodynamically active period (after 7.8 M Gorkha earthquake in 2015). For the rainfall event, DF contributed an average (± standard deviation) of 76 ± 10%, while AG and RT contributed equally with an average contribution of 10 ± 6% and 9 ± 8% respectively. Furthermore, posterior probability distributions of sediment sources during the period of frequent aftershocks (25 April - 30 May 2015) showed that the majority of sediment also originated from DF (74 ± 11 %), followed by AG (11 ± 7%) and RT (10 ± 9%).

3.3 Sediment contribution by sub-catchments using deconvolutional MixSIAR

The variability of $\delta^{13}C$-FAs and organic carbon for sediment sources and sediments of individual sub-catchments (Table 1) indicated that potential sediment sources have unique $\delta^{13}C$-FAs values (Fig. A.5 and Fig. A.6). Sediment source contributions for different tributaries of the Chitlang stream were estimated (Fig. 6) with source samples from the

401 respective tributary's sub-catchments. Source contributions were found to vary by sub-
402 catchment temporally. Sediment from the Dandakharka sub-catchment (M1, Fig. 1a)
403 originated from BLF (average contribution of 43, 31 and 25% in the early, mid and late wet
404 season, respectively), followed by RT-1 (27, 33, 33% in the early, mid and late wet season),
405 UP-E (10, 13, 14% in the early, mid and late wet season), MF (8, 11, 15 % in the early, mid
406 and late wet season), while other sources showed only minor contributions (<5%) (Fig. 6).
407 Sediment from the sub-catchment Kharka (M2, Fig. 1a) was dominated by MF 74, 87 and
408 75% during early, mid and late wet season, respectively. Mixing model estimation suggested
409 that sediment samples collected after the confluence of M1 and M2 i.e. M3 comprised overall
410 mean (± standard deviation) contributions of 74 ± 18, 78 ± 20 to 83 ± 17% during early, mid
411 and late wet-periods, respectively, from Dandakharka (M1) and 26 ± 18, 22 ± 17 to 17 ± 17%
412 during early, mid and late wet season, respectively, from Kharka (M2) (Table 4). Similar to
413 M2, Chhabugaun tributary sediment (M4, Fig. 1a) predominantly originated from MF
414 (average contribution 87, 95 and 87% during early, mid and late wet season, respectively).
415 The average contributions from the Upper-Chitlang (= M1 + M2) sub-catchments to sediment
416 samples collected after the Kapu confluence (M5, Fig. 1a) were 71, 64, to 74% during early,
417 mid and late wet seasons, respectively. Tributary sub-catchment contributions are generally in
418 agreement with catchment size, steepness and level of disturbance.

419 Combination of these sub-catchment estimates with the source contribution estimates for
420 each sub-catchment provides the basis for determining weighted sediment contributions for
421 M3, M5 and M6 within the D-MixSIAR framework. Three sources namely BLF, MF and RT-
422 1 almost equally contributed to M3 sediment: BLF contributed 32 ± 17, 24 ± 15 and 21 ± 13%
423 followed by MF by 25 ± 14, 27 ± 18 and 25 ± 16% and RT-1 by 20 ± 17, 26 ± 23 and 27 ±
424 24% during early, mid and late wet season, respectively. In contrast, for M5 sediment, MF
425 contributed to almost half of the sediment (43 ± 15, 52 ± 18, 41 ± 18% for early, mid and late

wet season, respectively), followed by an almost equal contribution from BLF (23 ± 12, 15 ± 11, 15 ± 11% for early, mid and late wet seasons, respectively) and RT-1 (14 ± 13, 17 ± 16, 20 ± 14% for early, mid and late wet season, respectively). In the case of the whole Chitlang catchment (M6), the majority of sediment originated from MF (41 ± 12, 47 ± 18, 38 ± 14% for early, mid and late wet season, respectively) with almost equal contributions from BLF (15 ± 8, 10 ± 7, 9 ± 7% for early, mid and late wet season, respectively), RT (11 ± 8, 7 ± 6, 10 ± 8% for early, mid and late wet season, respectively) and RT-1 (9 ± 8, 11 ± 10, 13 ± 12% for early, mid and late wet season, respectively), while LL, UP, PF and UP-E contributed the lowest amounts of sediment (Fig. 6, Fig. A.7). RT-1 was highest contributor in the upstream during mid and late-wet season and their contribution also gradually decreases downstream (Fig. A.7). The combined contributions from RT and RT-1 showed that unpaved road tracks were responsible for the second-largest proportion of M6 sediment after DF (BLF and MF). MF contributions gradually increased from upstream to downstream, while sediment contribution of BLF gradually decreased in the same direction (Fig. A.7). In most sediment, the 90% CI of source contributions showed wide ranges (this was especially true for RT-1, MF, BLF and UP-E), whereas the 90% CI of LL, RT, UP and PF were narrower (Fig. 6).

4 Discussion

4.1 Sediment source discrimination

Establishment of robust discrimination between δ^{13}C-FAs values of sediment sources is a key requirement for accurate source apportionment (Davis et al., 2015). An overlap was observed to some extent as well as source groups with large within-group variability (e.g. MF and RT, Fig. 4). This explains why mixing modelling yielded a high negative correlation between the contributions of these sources, irrespective of sediment types (Fig. A.4) and tracer sets. This was most notable between BLF and MF, and also between MF and RT. The

large negative correlation in posterior source contribution indicates that these sources are similar to each other in terms of tracer isotope values, which indicates that only one of both sources can actually contribute to the sediment mixture at a specific time (Stewart et al., 2015). Similar δ^{13}C-FA values were expected in BLF and MF, since MF is dominated by broadleaf and pine trees are relatively sparse in MF and thus less likely influence δ^{13}C-FA values. Soils under BLF and MF were characterised by δ^{13}C-FA values for C3 plants (Diefendorf et al., 2015). The LL and UP terraces are characterised by intense cultivation of varying crop types (i.e. cereal-legume/vegetable rotation) and soil management practices (tillage and farm yard manure (FYM) application), which may have caused high variation in δ^{13}C-FA values (Fig. A.2), especially due to mixing of C3 (rice, wheat, potato, beans) and C4 (maize, millet) plants. Removal of above ground biomass from agriculture fields is a common practice in the catchment. Instead of crop biomass, application of highly variable amounts of FYM, which is produced from crop biomass, leaf litter and pine needles, may introduce the isotopic signature of forest-derived FAs into agriculture fields and thereby lead to an increase in source variability (Jandl et al., 2007; Jandl et al., 2005). Additionally, LL receives sediment during flooding (Brown et al., 1999), which might also redistribute FA isotopic signatures from UP to LL. This is partially responsible for similar variation and overlapping source δ^{13}C-FAs values (Fig. A.2), despite the cultivation of plants with different photosynthetic pathways as major crops. Overlap and large within-source variability of δ^{13}C-FAs values of sources are considered important challenges in the application of isotope mixing models (Parnell et al., 2010). They are expected to result in an increased uncertainty in the estimated source contributions (Phillips and Gregg, 2001; Upadhayay et al., 2017). The a priori combination of sources (BLF and MF) as ‘deciduous forest’ gave similar results as the sum of the contributions of BLF and MF in the original analysis, i.e, posteriori aggregation of sources

(data not shown). This suggests that although the tracers are not able to discriminate between two functional sources, they can estimate their collective contribution to the sediment.

For both sediment types (suspended and streambed), the sediment source contributions did not change significantly when bulk $\delta^{13}C$ was added as an additional tracer (Fig. A.3). Despite the abundant use of soil and sediment bulk $\delta^{13}C$ in sediment tracing research (Collins et al., 2013; Fox and Ford, 2016; Fox and Martin, 2015; Fox and Papanicolaou, 2007; Laceby et al., 2015), there is no strong evidence that bulk soil $\delta^{13}C$ behaves conservatively (Collins et al., 2014; McCarney-Castle et al., 2017). The non-conservative behavior of bulk sediment C isotopes is possibly due to fractionation during organic matter decomposition (Benner et al., 1987; Fine and Carter, 2013). Furthermore, aquatic vegetation and freshwater autotrophs (e.g. algae) easily contaminate the sediment potentially altering the bulk isotope signature of the sediment, thereby confounding the interpretation of the source of eroded material. Despite these risks, several studies suggest the use of bulk isotopes as primary tracers in isotope mixing models during CSSI sediment source fingerprinting (Blake et al., 2012; Gibbs, 2008; Gibbs, 2013; Hancock and Revill, 2013). Our results suggest that bulk C isotopes should not be used in CSSI sediment source fingerprinting without evidence to support their conservative behavior.

4.2 Source contributions for different types of sediment

Both suspended and streambed sediment has been widely adopted in sediment source fingerprinting research (Collins et al., 2017; McCarney-Castle et al., 2017; Wilkinson et al., 2015). Bayesian modelling results supported the qualitative graphical analyses (Fig. 4) and also suggested DF (combined BLF and MF) as a primary source, with very small inter-seasonal variability in its relative contributions to suspended sediment compared to streambed sediment (Fig. 5). Differences in source composition between suspended and streambed

sediment have been reported in other studies (Koiter et al., 2013b; Lamba et al., 2015) that suggest both should be sampled to effectively understand sediment sources. However, variations in the estimated DF contribution to sediment types (Fig. 5) do not alter the broad conclusion that hillslope forest represents a primary sediment source within Chitlang catchment. Whilst this partial conclusion is based on the modelling of tracer data of generic (catchment-wide pooled) sediment sources and the plausible assumption that suspended sediment is dominated by newly delivered sediment from land surface sources (stream bed deposition and remobilisation of sediment is less likely in fast flowing mountain streams), sediment source apportionment within an individual sub-catchment should be considered to better understand the origin of sediment at a higher spatial resolution (section 4.3). Moreover, sediment core analysis from the reservoir could be used to predict the long-term variation of sediment source contributions, which is lacking in this study. Therefore, we concentrate on suspended sediments in the following section.

The sediment regime of the stream is not characterized by a constant sediment supply, but rather by the episodic occurrence of rainfall events and subsequent high stream flow. During high rainfall events, all catchment compartments may be actively connected to the mainstream (Bracken et al., 2015; Gomi et al., 2008). Given that sediment sources are well-connected to the stream, large events can transport sediment directly from eroded hillslopes and even flush previously deposited sediment (Le Gall et al., 2017). Hence, such event-based sediment samples provide robust information about sediment source hotspots at the catchment scale. Our estimations corroborated that DF is highly vulnerable to water erosion. Additionally, the 2015 Gorkha earthquake event might have damaged the steep hillslope surface of forested areas and subsequently triggered high sediment generation. The lack of landslides in the forest, the predominance of the bedrock dominated stream and relatively intact and dense vegetation cover during summer suggest that steep topography and high-

intensity rainfall might be major controlling physical factors for sediment generation and mobilization from the hillslope forested areas of this catchment.

4.3 Controls on sediment sources: land management activities

Despite the traditional view of a dominant sediment contribution from agricultural fields, Pooled-MixSIAR showed that agriculture contributed <5% to suspended sediments at the outlet of Chitlang stream (Fig. 5). Our results are in line with those of previous studies in the mid-hill catchments with terraced agriculture (Brown et al., 1999; Carver, 1997; Slaets et al., 2016). However, the Pooled-MixSIAR approach tends to average the variation of tracers of land uses located within different sub-catchments. Consequently, it provides source contribution results with high uncertainty. Furthermore, significant errors could be introduced if source groups are classified on the basis of catchment-wide generic sources alone in a catchment with heterogeneous vegetation and terrain (Pulley et al., 2017). In contrast, D-MixSIAR uses stratified source samples, which accounts for tracer variability of sources within individual sub-catchments and allows weighting of mixture proportions by sub-catchment contributions. The approach relies on the nested structure of the drainage network, therefore, reducing the complexity of tracer signatures of different sources within individual sub-catchments. As a result, within-source tracer variability decreased and discrimination of sources increased (Fig. A.8).

Combining total sub-catchment estimates with land use contributions computed for each tributary sub-catchment provides the basis for calculating weighted source contribution via D-MixSIAR along the catchment cascade (M3, M5, M6 sediment). We used D-MixSIAR to estimate land use contributions to suspended sediments. The contribution from BLF, RT-1 and UP-E decreased downstream (M3>M5>M6) as sediment transport distance from the location of the sources increases (Fig. A.7). The contribution of MF increased downstream

550 until M5 and remained stable towards the catchment outlet (M6). Based on D-MixSIAR, the
551 majority of sediment originated from MF, followed by BLF and RT-1 at the outlet of
552 catchment (Fig. 6, Fig.A.7), indicating that there is no *a priori* basis for assuming that
553 forested areas have inherently low rates of sediment generation even if forest land was
554 reported to have a low soil erodibility factor (Upadhayay et al., 2014). The increasing
555 contribution of MF along the sediment cascade can be explained by disturbed MF soil surface
556 on the steep slopes due to the impact of livestock grazing and collection of leaf litter using
557 hoe. D-MixSIAR results were consistent with the conceptual understanding of the catchment
558 (distribution of land use with slope gradient) and could be justified by the qualitative data. In
559 a survey of 150 households from an upstream village within the larger Kulekhani catchment
560 in 2013 (Panta et al., 2014), a majority (64%) of the farmers perceived that deforestation was
561 the main reason for soil erosion followed by road construction (28%), while only a minority
562 (2%) noted both unmanaged cropping pattern and stream bank erosion as major contributors
563 of sediments to the Kulekhani reservoirs.

564 Agriculture is predicted to be a minor source of sediment (mean contribution 15 - 20%)
565 input to the Chitlang stream network. The low contribution of agricultural terraces to the
566 sediment can probably be attributed to proper terrace maintenance and traditional irrigation
567 systems (Brown et al., 1999; Carver, 1997). Local farmers use back-sloping bench terraces for
568 upland agriculture with ditches around the terraces to direct the surface runoff out of the
569 upland terraces, thereby decreasing rill and ephemeral gully formation on agricultural fields.
570 In addition, most of the eroded soil from upland terraces is finally transferred to irrigated
571 lowland terraces through run-on as well as through irrigation water and deposited on the
572 irrigated terraces as well as the canal bed. Carver (1997) estimated an accumulation of 6.6
573 mm $year^{-1}$ of eroded material on the irrigated terraces in the mid-hills of Nepal. The authors
574 observed that deposited sediment was frequently cleaned from irrigation canals. Thus,

irrigation canals and terracing slow down sediment transfer and result in upstream accumulation of sediment on the valley floor and lowland terrace, forming local net sediment sink zones modifying the sediment dynamics at the catchment scale (Brown et al., 1999; Carver, 1997).

D-MixSIAR results showed that forests (BLF and MF) were the primary sediment source during all seasons while unpaved road tracks represented a major secondary sediment source within the Chitlang catchment. Soil erosion in the forest might be exacerbated by the combination of surface disturbance (e.g. leaf litter collection activities), high rainfall intensity, seasonally dry periods, forest fires and naturally dynamic landscapes. The short-duration, high-intensity monsoon storms that are common in the catchment provide the required rainfall erosivity to initiate surface erosion on steeper slopes (Bookhagen, 2010; Karki et al., 2017). Farmers collect leaf litter using hand racking, harvest timber and graze livestock (cows and goats) in the forest, which makes the forest floor bare or disturbed. Gardner and Gerrard (2002) suggested that ground cover is more important than canopy cover in reducing runoff and water erosion in the mid-hill forest. The average rate of soil loss and the contribution to total soil loss from steeper slopes are tremendously high compared with that from gentle slopes (Bahadur, 2012; Garcia-Ruiz et al., 2015; Su et al., 2016). Moreover, unfortified dirt roads located inside the broadleaf forest are highly vulnerable to erosion due to rutted surfaces. Most of the rural roads in the mid-hills are unpaved and poorly maintained without roadside drainage systems, leading to concentrated flow, resulting in soil erosion (Merz et al., 2006; Su et al., 2016). Additional tracers such as fallout radionuclides may provide further insight into the major erosion processes generating sediment from different land uses, which is lacking in this study. Notwithstanding, the continued supply of sediment from forests will result in rapid siltation of the reservoir and loss of ecosystem services that consequently result in shortened economic returns from the reservoir. Thus, in order to protect the catchment from degradation,

forests should be better managed. However, since decisions to protect the forests are enforced by the community forest user groups (CFUs), the planning of effective measures for soil conservation in the forests should target a 'bottom-up' approach. This should ideally involve the integration of CFUs in a framework of paying for ecosystem services, performance-based disbursement of electricity revenue to local communities, and effective monitoring of forest and other developmental activities (e.g. road construction) across the catchment.

5 Conclusions

The stable carbon isotopic composition of long-chain saturated FAs (δ^{13}C-FA) associated with soil of various land uses and different types of stream sediment (bed, suspended, event) were used as input for a Bayesian mixing model to estimate the spatio-temporal variation in land use-specific sediment source contributions to the Chitlang stream located in the mid-hills of Nepal. We showed that applying catchment-wide (generic) sources cannot explain the sediment transport within the catchment because sediment delivery from the different sources is sub-catchment specific due to localized changes in gradient, ground cover, vegetation and microtopography in the mountaneous catchments. Application of a deconvolutional framework to MixSIAR (D-MixSIAR) strongly enhanced our understanding of the relatively complex patterns of sediment contributions to different tributaries representing sub-catchments along the mainstream. This study showed that the largest sources of sediment in Chitlang catchment were mixed forest (MF) (41 ± 13%) and broadleaf forest (BLF) (15 ± 8%) followed by unpaved rural road tracks on flat (11 ± 8%) and steep lands (9 ±7%) during early wet season (the time of highest risk for soil erosion by water in the mid-hills of Nepal). The effect of temporal hydrological variability on the land use contributions was not significant. Clearly, sediment sources showed high spatial variation along the Chitlang stream sediment

cascade because of spatial changes in topography and land use management. Prediction of source contributions was improved by a categorization of sources for each sub-catchment and estimation of a total, weighted source contribution using sub-catchment contributions.

Overall this study showed that community managed forest is the major primary, and road tracks are dominant secondary sources of sediments at the different locations of Chitlang stream. The estimates of agricultural terraces contribution are significantly lower compared to forest throughout the year. It is acknowledged that D-MixSIAR is still a black-box model that provides no information on the internal processes, or secondary sediment sources and sinks within the catchment. Therefore, without spatially explicit sediment loading data, proportions must still be compared with some caution. Nevertheless, management of forests and unpaved roads in the Chitlang catchment should be an essential component of the strategies to control sediment inputs to Kulekhani reservoir. Hence, there is a need for better coordination among community forest user groups and provision of hydroelectricity revenue in return for forest conservation measures.

Acknowledgements

This work was financially supported by Vlaamse Inter-universitaire Raad (VLIR) Belgium as a part of an ICP-PhD grant. Special thank is expressed to the Horizon 2020, RISE IMIXSED (Integrating isotopic techniques with Bayesian modelling for improved assessment and management of global sedimentation problems) project for MixSIAR training. We are very grateful for the comments made by the anonymous reviewer and we believe that they have helped us to significantly improve the manuscript.

References

Acharya GP, Tripathi BP, Gardner RM, Mawdesley KJ, McDonald MA. Sustainability of sloping land cultivation systems in the mid-hills of Nepal. Land Degradation & Development 2008; 19: 530-541.

Bahadur KCK. Spatio-temporal patterns of agricultural expansion and its effect on watershed degradation: a case from the mountains of Nepal. Environmental Earth Sciences 2012; 65: 2063-2077.

Benner R, Fogel ML, Sprague EK, Hodson RE. Depletion of C-13 in lignin and its implications for stable carbon isotope studies. Nature 1987; 329: 708-710.

Blake WH, Ficken KJ, Taylor P, Russell MA, Walling DE. Tracing crop-specific sediment sources in agricultural catchments. Geomorphology 2012; 139: 322-329.

Bookhagen B. Appearance of extreme monsoonal rainfall events and their impact on erosion in the Himalaya. Geomatics Natural Hazards & Risk 2010; 1: 37-50.

Bracken LJ, Turnbull L, Wainwright J, Bogaart P. Sediment connectivity: a framework for understanding sediment transfer at multiple scales. Earth Surface Processes and Landforms 2015; 40: 177-188.

Brown S, Schreier H, Shah PB, Lavkulich LM. Modelling of soil nutrient budgets: an assessment of agricultural sustainability in Nepal. Soil Use and Management 1999; 15: 101-108.

Carver M. Diagnosis of Headwater Sediment Dynamics in Nepal's Middle Mountains: Implications for Land Management. PhD thesis. University of British Columbia, Vancouver, Canada, 1997.

Collins AL, Pulley S, Foster IDL, Gellis A, Porto P, Horowitz AJ. Sediment source fingerprinting as an aid to catchment management: a review of the current state of knowledge and a methodological decision-tree for end-users. Journal of Environmental Management 2017; 194: 86-108.

Collins AL, Williams LJ, Zhang YS, Marius M, Dungait JAJ, Smallman DJ, Dixon ER, Stringfellow A, Sear DA, Jones JI, Naden PS. Catchment source contributions to the sediment-bound organic matter degrading salmonid spawning gravels in a lowland river, southern England. Science of The Total Environment 2013; 456–457: 181-195.

Collins AL, Williams LJ, Zhang YS, Marius M, Dungait JAJ, Smallman DJ, Dixon ER, Stringfellow A, Sear DA, Jones JI, Naden PS. Sources of sediment-bound organic matter infiltrating spawning gravels during the incubation and emergence life stages of salmonids. Agriculture Ecosystems & Environment 2014; 196: 76-93.

Cooper RJ, Krueger T, Hiscock KM, Rawlins BG. High-temporal resolution fluvial sediment source fingerprinting with uncertainty: a Bayesian approach. Earth Surface Processes and Landforms 2015; 40: 78-92.

Davis P, Syme J, Heikoop J, Fessenden-Rahn J, Perkins G, Newman B, Chrystal AE, Hagerty SB. Quantifying uncertainty in stable isotope mixing models. Journal of Geophysical Research-Biogeosciences 2015; 120: 903-923.

Dhital MR. Geology of the Nepal Himalaya: regional perspective of the classic collided Orogen. London: Springer, 2015.

Diefendorf AF, Leslie AB, Wing SL. Leaf wax composition and carbon isotopes vary among major conifer groups. Geochimica Et Cosmochimica Acta 2015; 170: 145-156.

Dijkshoorn K, Huting J. Soil and terrain database for Nepal. Report No: Report 2009/01, (available through: http://www.isric.org), ISRIC–World Soil Information, Wageningen, The Netherland (29 p. with data set). 2009.

695 Fine ST, Carter BJ. Effect of Sedimentation on Soil Organic Carbon Content and delta 13C
696 Values After 7 Years of Burial. Soil Science 2013; 178: 647-653.
697 Fox JF, Ford WI. Impact of landscape disturbance on the quality of terrestrial sediment
698 carbon in temperate streams. Journal of Hydrology 2016; 540: 1030-1042.
699 Fox JF, Martin DK. Sediment fingerprinting for calibrating a soil erosion and sediment-yield
700 model in mixed land-use watersheds. Journal of Hydrologic Engineering 2015; 20:
701 C4014002-1
702 Fox JF, Papanicolaou AN. The use of carbon and nitrogen isotopes to study watershed erosion
703 processes. Journal of the American Water Resources Association 2007; 43: 1047-1064.
704 Garcia-Ruiz JM, Begueria S, Nadal-Romero E, Gonzalez-Hidalgo JC, Lana-Renault N,
705 Sanjuan Y. A meta-analysis of soil erosion rates across the world. Geomorphology
706 2015; 239: 160-173.
707 Gardner RAM, Gerrard AJ. Relationships between runoff and land degradation on non-
708 cultivated land in the Middle Hills of Nepal. International Journal of Sustainable
709 Development and World Ecology 2002; 9: 59-73.
710 Gardner RAM, Gerrard AJ. Runoff and soil erosion on cultivated rainfed terraces in the
711 Middle Hills of Nepal. Applied Geography 2003; 23: 23-45.
712 Gibbs MM. Identifying source soils in contemporary estuarine sediments: a new compound-
713 specific isotope method. Estuaries and Coasts 2008; 31: 344-359.
714 Gibbs MM. Protocols on the use of the CSSI technique to identify and apportion soil sources
715 from land use Report No: HAM2013-106, National Institute of Water and
716 Atmospheric Research Ltd, Hamilton, New Zealand. 2013.
717 Gomi T, Sidle RC, Miyata S, Kosugi K, Onda Y. Dynamic runoff connectivity of overland
718 flow on steep forested hillslopes: Scale effects and runoff transfer. Water Resources
719 Research 2008; 44: W08411.
720 GoN/EbA/UNDP. Development of Ecosystem based Sediment Control Techniques and
721 Design of Siltation Dam to Protect Phewa Lake. Report No, Summary Report.
722 Prepared By Forum for Energy and Environment Development (FEED) P. Ltd. for
723 The Ecosystem Based Adaptation in Mountain Ecosystems (EbA) Nepal Project.
724 Government Of Nepal, United Nations Environment Programme, United Nations
725 Development Programme, International Union For Conservation Of Nature, and the
726 German Federal Ministry for the Environment, Nature Conservation, Building And
727 Nuclear Safety. 2015.
728 Griepentrog M, Eglinton TI, Hagedorn F, Schmidt MWI, Wiesenberg GLB. Interactive
729 effects of elevated CO_2 and nitrogen deposition on fatty acid molecular and isotope
730 composition of above- and belowground tree biomass and forest soil fractions. Global
731 Change Biology 2015, 21: 473-486.
732 Hancock GJ, Revill AT. Erosion source discrimination in a rural Australian catchment using
733 compound-specific isotope analysis (CSIA). Hydrological Processes 2013; 27: 923-
734 932.
735 Hardy F, Bariteau L, Lorrain S, Theriault I, Gagnon G, Messier D, Rougerie JF. Geochemical
736 tracing and spatial evolution of the sediment bed load of the Romaine River, Quebec,
737 Canada. Catena 2010; 81: 66-76.
738 Huberty CJ, Olejnik S. Applied MANOVA and Discriminant Analysis: Wiley, 2006.
739 Ichihara K, Fukubayashi Y. Preparation of fatty acid methyl esters for gas-liquid
740 chromatography. Journal of Lipid Research 2010; 51: 635-640.
741 Jackson A. SIBER. Web https://github.com/AndrewLJackson/SIBER. Accessed. 15 July,
742 2016.

743 Jandl G, Leinweber P, Schulten HR. Origin and fate of soil lipids in a Phaeozem under rye
744 and maize monoculture in Central Germany. Biology and Fertility of Soils 2007; 43:
745 321-332.
746 Jandl G, Leinweber P, Schulten HR, Ekschmitt K. Contribution of primary organic matter to
747 the fatty acid pool in agricultural soils. Soil Biology & Biochemistry 2005; 37: 1033-
748 1041.
749 Karki R, ul Hasson S, Schickhoff U, Scholten T, Bohner J. Rising Precipitation Extremes
750 across Nepal. Climate 2017; 5: 4.
751 Koiter AJ, Lobb DA, Owens PN, Petticrew EL, Tiessen KHD, Li S. Investigating the role of
752 connectivity and scale in assessing the sources of sediment in an agricultural
753 watershed in the Canadian prairies using sediment source fingerprinting. Journal of
754 Soils and Sediments 2013a; 13: 1676-1691.
755 Koiter AJ, Owens PN, Petticrew EL, Lobb DA. The behavioural characteristics of sediment
756 properties and their implications for sediment fingerprinting as an approach for
757 identifying sediment sources in river basins. Earth-Science Reviews 2013b; 125: 24-
758 42.
759 Laceby JP, Olley J, Pietsch TJ, Sheldon F, Bunn SE. Identifying subsoil sediment sources
760 with carbon and nitrogen stable isotope ratios. Hydrological Processes 2015; 29: 1956-
761 1971.
762 Lamba J, Karthikeyan KG, Thompson AM. Apportionment of suspended sediment sources in
763 an agricultural watershed using sediment fingerprinting. Geoderma 2015; 239: 25-33.
764 Le Gall M, Evrard O, Foucher A, Laceby JP, Salvador-Blanes S, Maniere L, Lefevre I,
765 Cerdan O, Ayrault S. Investigating the temporal dynamics of suspended sediment
766 during flood events with Be-7 and Pb-210(xs) measurements in a drained lowland
767 catchment. Scientific Reports 2017; 7: 42099
768 McCarney-Castle K, Childress TM, Heaton CR. Sediment source identification and load
769 prediction in a mixed-use Piedmont watershed, South Carolina. Journal of
770 Environmental Management 2017; 185: 60-69.
771 McFerrin L. HDMD: Statistical analysis tools for high dimention molecular data (HDMD). R
772 package version 1.2. https://CRAN.R-project.org/package=HDMD 2013.
773 Merz J. Water balances, floods and sediment transport in the Hindu Kush-Himalayas. Web
774 http://lib.icimod.org/record/7484. Accessed. 22 March, 2017.
775 Merz J, Dangol PM, Dhakal MP, Dongol BS, Nakarmi G, Weingartner R. Road construction
776 impacts on stream suspended sediment loads in a nested catchment system in Nepal.
777 Land Degradation & Development 2006; 17: 343-351.
778 Mukundan R, Walling DE, Gellis AC, Slattery MC, Radcliffe DE. Sediment source
779 fingerprinting: transforming from a research tool to a management tool. Journal of the
780 American Water Resources Association 2012; 48: 1241-1257.
781 NEA. A Year in review-fiscal year 2015/2016. Report No, Nepal Electricity Authority,
782 Kathmandu, Nepal. 2016.
783 Panta D, Rao N, Upadhayay SN, Karky BS. Benefit sharing mechanisms in hydropowr
784 projects: Lessons from Nepal and India. In: Vaidya RA, Sharma E, editors. Research
785 Insights on climate and water in the Hindu Kush Himalayas. ICIMOD, Kathmandu,
786 Nepal 2014.
787 Parnell AC, Inger R, Bearhop S, Jackson AL. Source partitioning using stable isotopes:
788 coping with too much variation. PLoS One 2010; 5: e9672.
789 Phillips DL, Gregg JW. Uncertainty in source partitioning using stable isotopes. Oecologia
790 2001; 127: 171-179.

Phillips JM, Russell MA, Walling DE. Time-integrated sampling of fluvial suspended sediment: a simple methodology for small catchments. Hydrological Processes 2000; 14: 2589-2602.

Pulley S, Foster I, Collins AL. The impact of catchment source group classification on the accuracy of sediment fingerprinting outputs. Journal of Environmental Management 2017; 194: 16-26.

Semmens BX, Ward EJ, Moore JW, Darimont CT. Quantifying inter- and intra-population niche variability using hierarchical Bayesian stable isotope mixing models. PLoS One 2009; 4: e6187.

Shrestha HS. Sedimentation and sediment handling in himalayan reservoirs. Department of Hydraulics and Environmental Engineering. PhD thesis. Norwegian University of Science and Technology, Trondheim, Norway, 2012, pp. 236.

Slaets JIF, Schmitter P, Hilger T, Hue DTT, Piepho HP, Vien TD, Cadisch G. Sediment-associated organic carbon and nitrogen inputs from erosion and irrigation to rice fields in a mountainous watershed in Northwest Vietnam. Biogeochemistry 2016; 129: 93-113.

Stewart HA, Massoudieh A, Gellis A. Sediment source apportionment in Laurel Hill Creek, PA, using Bayesian chemical mass balance and isotope fingerprinting. Hydrological Processes 2015; 29: 2545-2560.

Sthapit KM, Balla MK. Review of runoff and soil loss studies: A teching material. Institute of forestry (IOF), Pokhara, Nepal, 1998.

Stock BC, Semmens BX. MixSIAR GUI User Manuel. Version 3.1. Web https://github.com/brianstock/MixSIAR/. Accessed. 26 February, 2016.

Su Z-a, Xiong D-h, Deng W, Dong Y-f, Ma J, Padma CP, Gurung BS. 137Cs tracing dynamics of soil erosion, organic carbon, and total nitrogen in terraced fields and forestland in the Middle Mountains of Nepal. Journal of Mountain Science 2016; 13: 1829-1839.

Tiwari KR, Sitaula BK, Bajracharya RM, Borresen T. Runoff and soil loss responses to rainfall, land use, terracing and management practices in the Middle Mountains of Nepal. Acta Agriculturae Scandinavica Section B-Soil and Plant Science 2009; 59: 197-207.

Upadhayay HR, Bodé S, Griepentrog M, Bajracharya RM, Blake W, Cornelis W, Boeckx P. Isotope mixing models require individual isotopic tracer content for correct quantification of sediment source contributions. Hydrological Processes 2018; 32: 981-989.

Upadhayay HR, Bodé S, Griepentrog M, Huygens D, Bajracharya RM, Blake WH, Dercon G, Mabit L, Gibbs M, Semmens BX, Stock BC, Cornelis W, Boeckx P. Methodological perspectives on the application of compound-specific stable isotope fingerprinting for sediment source apportionment. Journal of Soils and Sediments 2017; 17: 1537-1553.

Upadhayay HR, Gajurel S, Bajaracharya RM, Cornelis W, Boeckx P. Effect of land use on soil degradation in Chitlang watershed of Nepal. Forestry (Journal of Institute of Forestry, Nepal) 2014; 14: 28-41.

Vale SS, Fuller IC, Procter JN, Basher LR, Smith IE. Application of a confluence-based sediment-fingerprinting approach to a dynamic sedimentary catchment, New Zealand. Hydrological Processes 2016; 30: 812-829.

Venables WN, Ripley BD. Modern applied statistics with S. New York: Springer, 2002.

Vercruysse K, Grabowski RC, Rickson RJ. Suspended sediment transport dynamics in rivers: Multi-scale drivers of temporal variation. Earth-Science Reviews 2017; 166: 38-52.

von Westarp S, Schreier H, Brown S, Shah RB. Agricultural intensification and the impacts on soil fertility in the Middle Mountains of Nepal. Canadian Journal of Soil Science 2004; 84: 323-332.
Walling DE. The evolution of sediment source fingerprinting investigations in fluvial systems. Journal of Soils and Sediments 2013; 13: 1658-1675.
Wilkinson SN, Olley JM, Furuichi T, Burton J, Kinsey-Henderson AE. Sediment source tracing with stratified sampling and weightings based on spatial gradients in soil erosion. Journal of Soils and Sediments 2015; 15: 2038-2051.

Tables

Table 1 Characteristics of sediment sampling locations (see Fig. 1) and potential sediment sources (broad leaf forest (BLF), mixed forest (MF), pine forest (PF), encroached upland terraces into BLF (UP-E), upland terraces (UP), lowland terraces (LL)), unpaved road tracks on slopes inside BLF (RT-1) and unpaved road tracks on flatter areas (RT)).

Table 2 Mahalanobis distances between group centroids (see Fig. 4) and reliability of source discrimination analysis using $\delta^{13}C$ of long-chain saturated fatty acids (C_{22}-C_{32}). Significant effects are in bold. Sources: broad leaf forest (BLF), mixed forest (MF), pine forest (PF), upland terraces (UP), lowland terraces (LL), unpaved road tracks (RT).

Table 3 Sediment source apportionment after a high rainfall event (14 to15 August, 2014) and aftershocks following the Gorkha earthquake (7.8 M) on 25 April 2015. Abbreviations: deciduous forest (DF), broad leaf forest (BLF), mixed forest (MF), combined agriculture terraces (AG), lowland terraces (LL), upland terraces (UP), pine forest (PF), unpaved road tracks (RT).

Table 4 Estimated relative contribution of each tributary sub-catchments (M1 = Dandakharka, M2 = Kharka, M3 =Upper-Chitlang and M4= Chhabugaun) to the confluence-sediment (M3, M5) for early, mid and late wet season. For details see Figures 1 and 6. Mean ± standard deviation with 90% credible intervals in parenthesis.

Figures

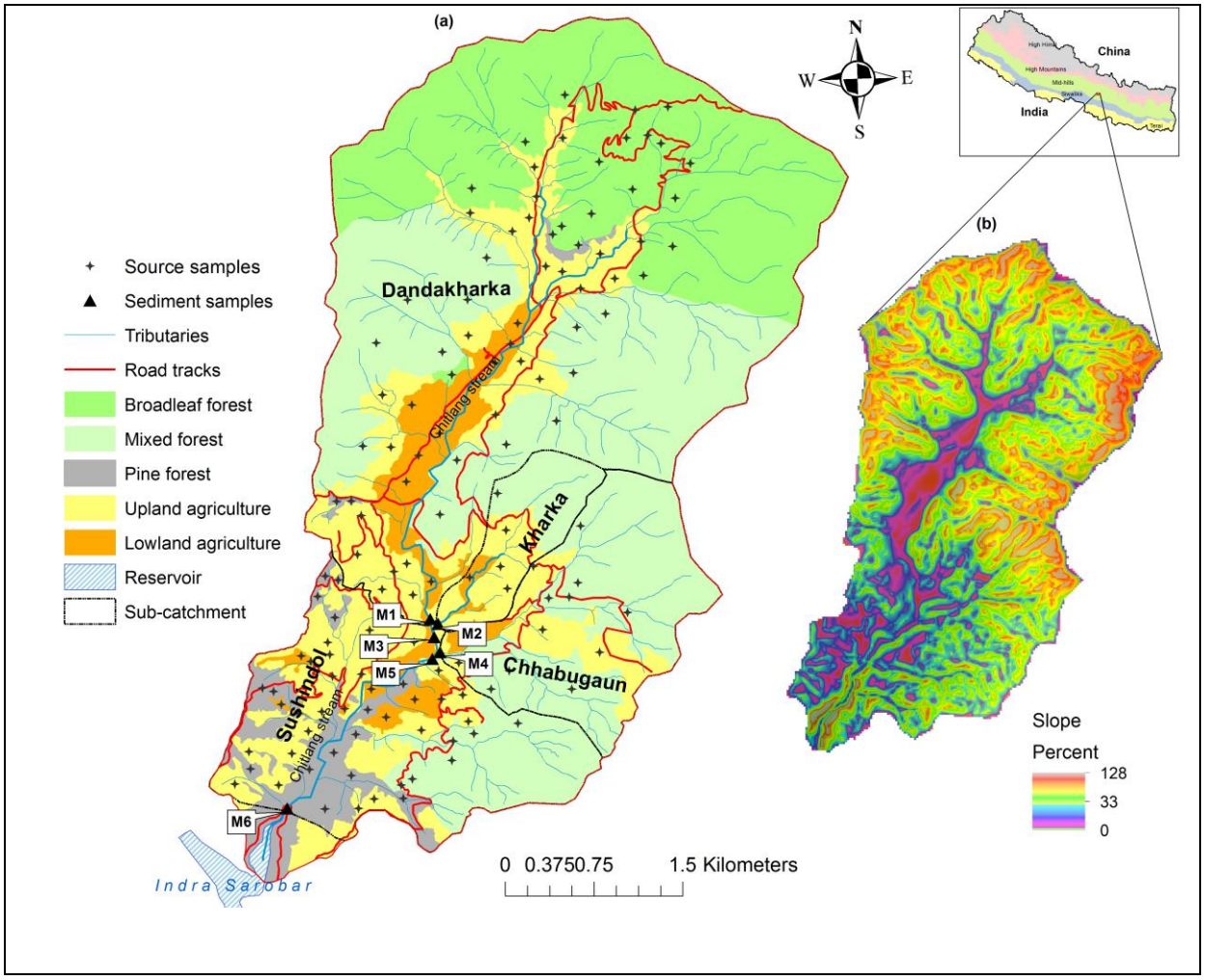

Fig. 1 Chitlang catchment in the mid-hills of Nepal (upper-right inset) (a) sub-catchments, land use and land cover distributions (digitized from **Google Earth**) with source and sediment (M1, M2, M3, M4, M5 and M6) sampling locations, and (b) slope map of the study area obtained from digitized map layers of topographic map published by the Department of Survey, Government of Nepal (1996).

Fig. 2 Source soil and sediment sampling in the Chitlang catchment, (a) mixed rain-fed and irrigated farming on terraces (middle) and mixed forest on steep slopes (left and right), (b) stream bed sediment sampling with flat trowel and (c) installed time-integrated mass-flux sampler (TIMS) at the outlet of the Chitlang stream.

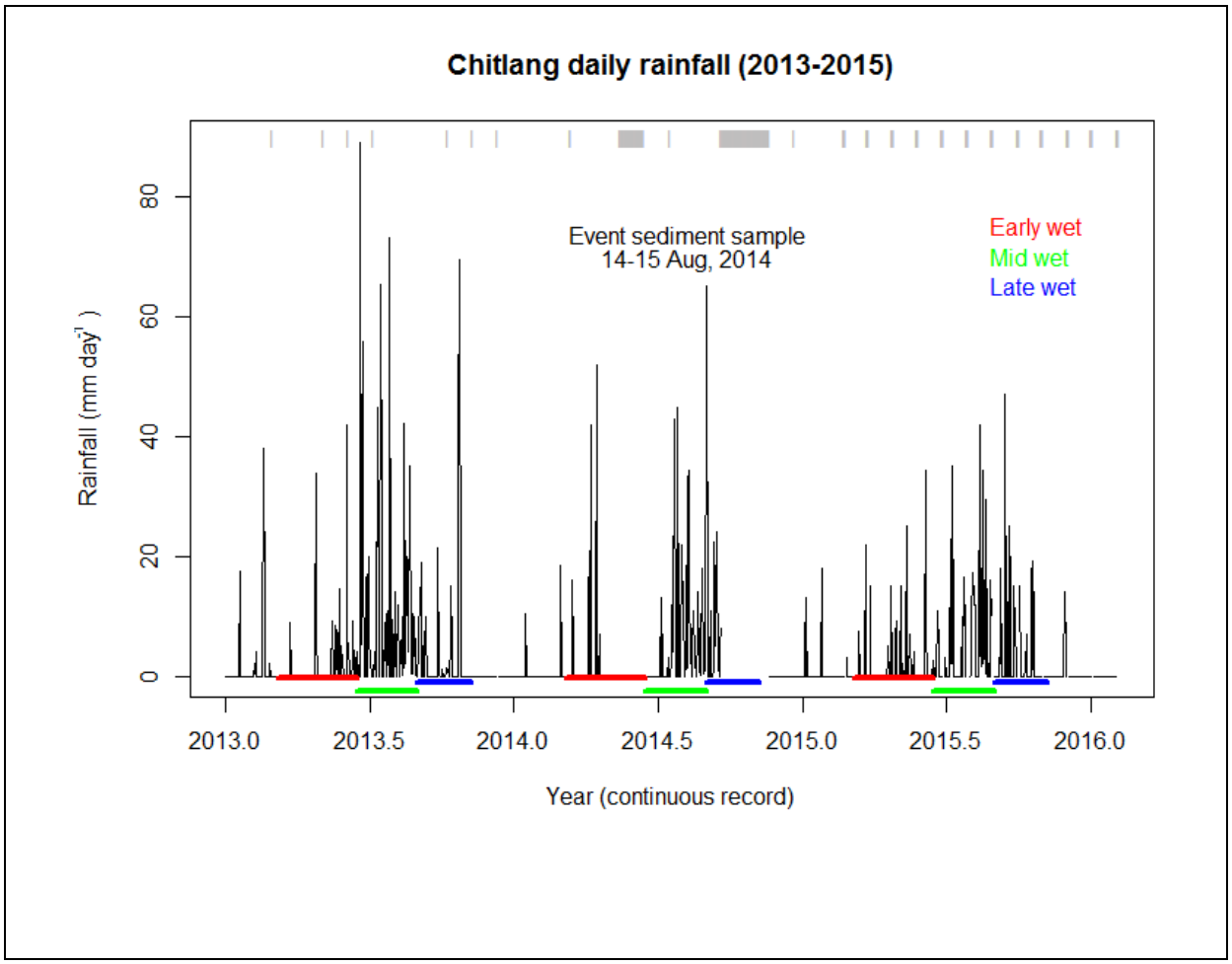

900

901 Fig. 3 Rainfall distribution in Markhu station (Index no. 0915, Department of Hydrology and
902 Meteorology, Government of Nepal) at the outlet of Chitlang catchment. Horizontal gray bars
903 on top represent missing rainfall data while bottom horizontal bars represent sediment
904 sampling periods (red = early wet, green = mid wet and blue = late wet periods).

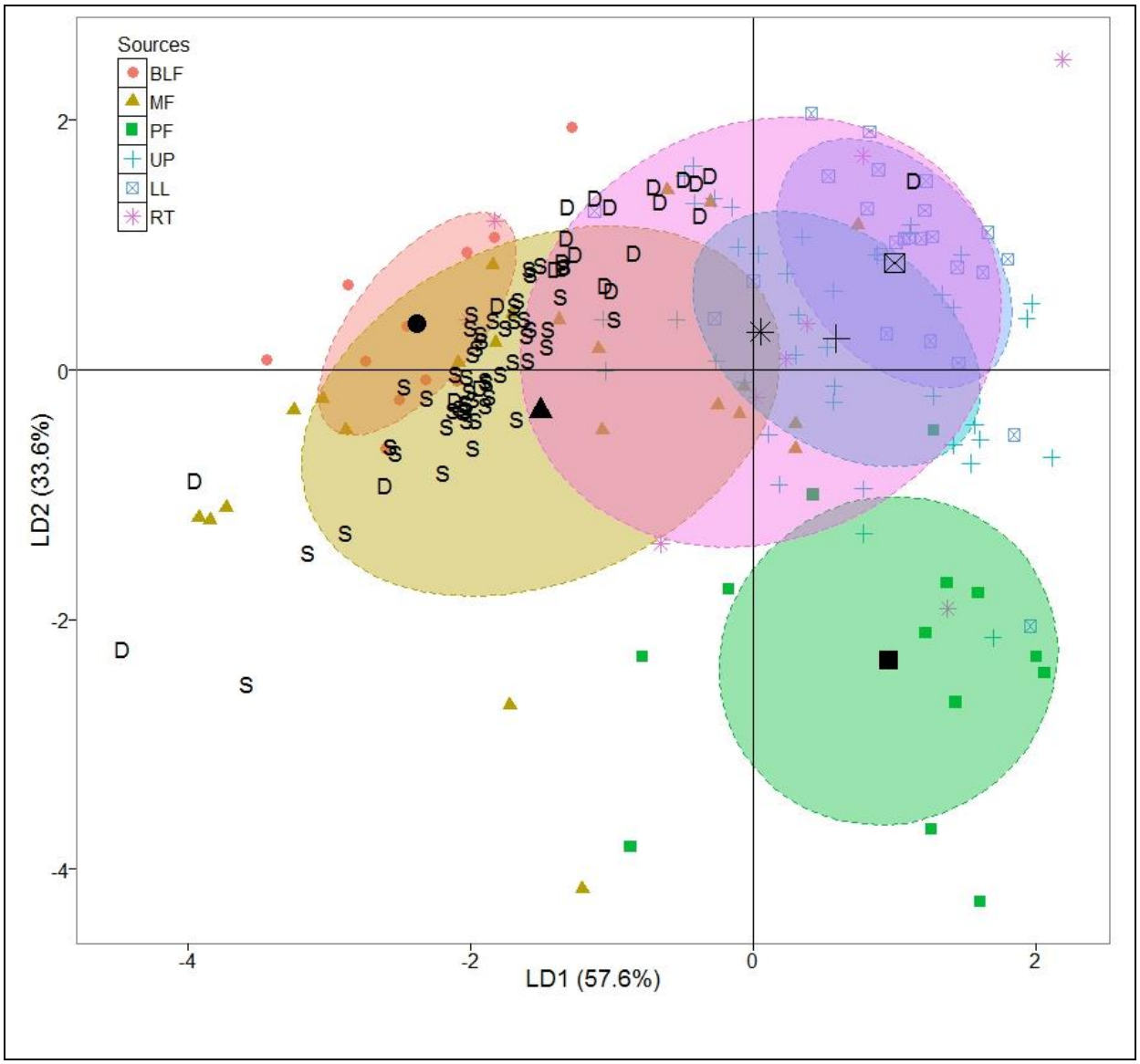

905

906 Fig. 4 Discriminant analysis (DA) of generic sediment sources using $\delta^{13}C$ of saturated long-
907 chain fatty acids (C_{22}-C_{32}) with projection of sediment samples (S = suspended and D =
908 stream bed) on the LDA scatter plot. Shaded ellipsoids encompass 50% of group variability.
909 Sources: broad leaf forest (BLF), mixed forest (MF), pine forest (PF), upland terraces (UP),
910 lowland terraces (LL), unpaved road tracks (RT).

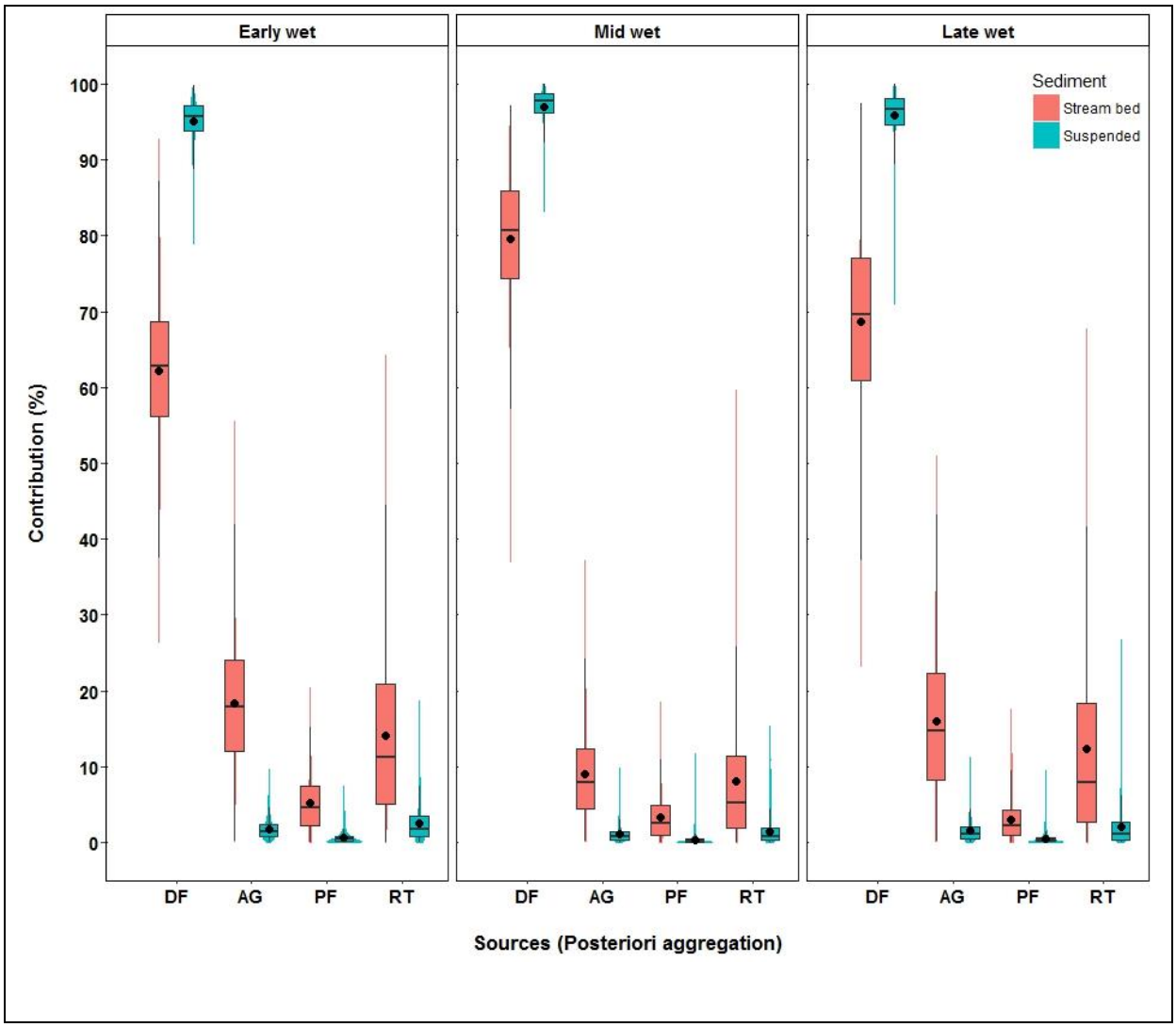

911

912 Fig. 5 Source contributions to streambed and suspended sediments at the catchment outlet
913 estimated based on $\delta^{13}C$ FA tracers (C_{22} - C_{32}) using concentration-dependent pooled-
914 MixSIAR model. Box plots with solid circle representing the average contribution. Sources:
915 deciduous forest (DF), agricultural terraces (AG), pine forest (PF) and unpaved road tracks
916 (RT).

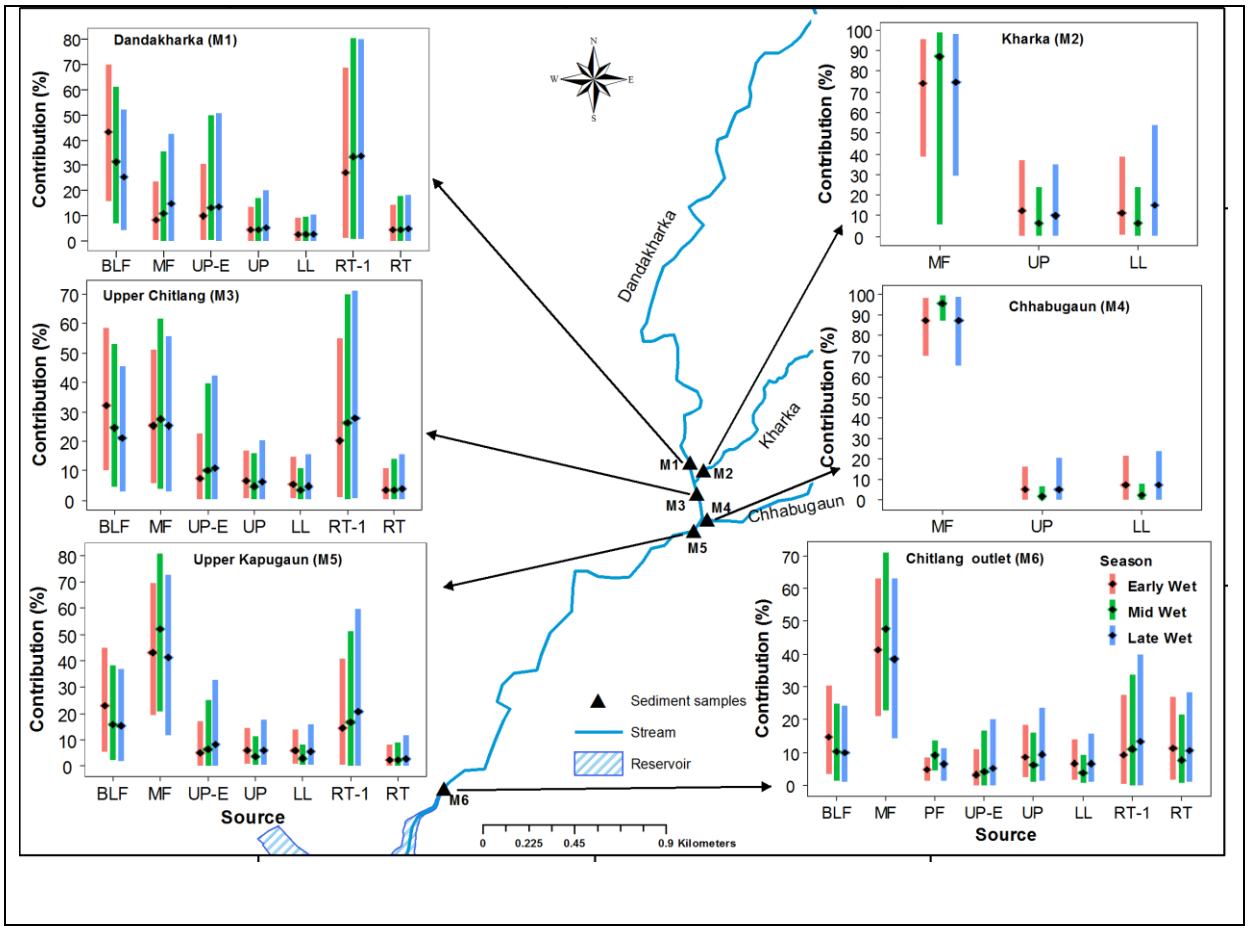

Fig. 6 Mean relative contribution (%) of sediment sources estimated with deconvolutional MixSIAR using confluence-based suspended sediment collected before and after confluences at different tributaries of Chitlang stream. Vertical bars represent 90% credible intervals and the middle point (black diamond) represents the average contribution, while seasons are given in different colours. Sources: broadleaf forest (BLF), mixed forest (MF), pine forest (PF), encroached upland terraces into BLF (UP-E), upland terraces (UP), lowland terraces (LL), unpaved road tracks on slope inside BLF (RT-1) and unpaved road tracks on flat terrain (RT).